

# Nonlinear multivariate curve resolution alternating least squares (NL-MCR-ALS)<sup>†</sup>

Alexey L. Pomerantsev<sup>a,b,\*</sup>, Yuri V. Zontov<sup>c</sup> and Oxana Ye. Rodionova<sup>a</sup>

**Bilinearity is the basic principle of multivariate curve resolution. In this paper, we consider a case when this premise is violated. We demonstrate that the alternating least squares approach can still be used to solve the problem. The developed theory is applied to calibration of spectral data that includes the so-called saturated peaks, which are flattened because of samples with ultrahigh absorbance. We demonstrate that in spite of serious violations of the Lambert–Beer law, the results of prediction are quite satisfactory, and the accuracy is better than in other competing methods. Copyright © 2014 John Wiley & Sons, Ltd.**

**Keywords:** MCR; ALS; nonlinearity, peak saturation; Lambert–Beer law violations; nitric acid

## 1. INTRODUCTION

Quantitative determination of analytes in mixtures by means of spectroscopy together with chemometric data processing is an approach widely used both in analytical laboratories and at manufacturing sites of food and pharmaceutical industries, chemical plants, and so on. Ultraviolet–visible (UV–Vis) and near infrared spectrometry are well adapted for the in-line and on-line control, and thus, they are employed in different process analytical technology (PAT) solutions [1]. The multivariate calibration methods such as the partial least squares (PLS) regression and its numerous modifications [2] are the most popular and well-established techniques. These methods yield a prediction of an analyte concentration without reconstruction of the pure spectra of the mixture's components. Another class of methods involves a two-step approach. First, it aims at a reconstruction of spectroscopic data; afterwards, it uses the spectroscopic profiles to solve the quantitative calibration problem. The multivariate curve resolution alternating least squares (MCR-ALS) method belongs to the latter class [3]. In application of MCR-ALS to calibration problems, special attention is directed at the employment of various types of constraints. Such constraints include those that carry significant chemical/physical information and help to avoid ambiguity of the result. In recent works, correlation constraints were also employed to account for such side effects as material aging, matrix effects, and temperature changes [4,5].

There are several studies that compare the performance of PLS and MCR-ALS for the calibration of complex mixtures. The results show that both methods generate comparable predictions [5–7]. Despite the fact that the MCR-ALS computational procedure is more complex, the additional information regarding the pure spectra shapes, acquired in the course of this procedure, is valuable to understand the processes under investigation. The assumption of a bilinear relation between the experimental data and the concentration of the components/pure spectra is in the background of both methods.

Process control is often the ultimate purpose of the developed calibration models. No doubt that a laboratory-scale calibration model should be sufficiently secure to be transferred to

plant-scale implementation. During the transfer, the following circumstances should be taken into account. First, the concentrations in real life production could be occasionally out of the range studied in the laboratory. Therefore, the model should be, to some extent, stable in the case of a prediction out of the explored concentration range. Second, the absorbance of some analytes may be very high. As a result, the corresponding peaks become distorted and flattened [8]. This effect can be viewed as an apparent violation of the Lambert–Beer law, as concentration increases, but the corresponding peak's height remains unchanged. Sometimes, such peak distortions are wrongly called detector saturation. On the contrary, the transmittance signal is very low in highly absorptive media. Therefore, we prefer to use the term *peak saturation* in relation to a peak that is flattened because of ultrahigh absorbance. There are many ways to avoid such situations in a laboratory, for example, by means of sample dilution, shortening of the optical path length, or, where possible, changing a spectral region. In PAT applications, such methods are not always available.

Sometimes, we have to analyze mixtures of analytes characterized by very high and very low extinction coefficients simultaneously. Reduction of the optical path length makes the determination of the components with low absorptivity

\* Correspondence to: Alexey L. Pomerantsev, Semenov Institute of Chemical Physics, RAS, Kosygin str. 4, 119991, Moscow, Russia.  
E-mail: forecast@chph.ras.ru

<sup>†</sup> Presented at the Ninth Annual Winter Symposium on Chemometrics (WSC-9), Tomsk, Russia, February 17–21, 2014.

a A. L. Pomerantsev, O. Y. Rodionova  
Semenov Institute of Chemical Physics, RAS, Kosygin str. 4, 119991, Moscow, Russia

b A. L. Pomerantsev  
Institute of Natural and Technical Systems, RAS, Kurortny pr. 99/18, 354024, Sochi, Russia

c Y. V. Zontov  
National Research University 'Higher School of Economics', Myasnitskaya 20, 101000, Moscow, Russia

impossible, while an increase of the optical path length causes peak saturation for the highly absorptive component. Thus, we face a challenge of quantitative determination of a mixture's components when bilinearity between spectral data and concentrations/pure spectra does not hold. Claiming violation of bilinearity, we bear in mind that, in general, the investigated mixture is subject to the Lambert–Beer law. Had we had an 'ideal' instrument, the bilinearity would have been kept. However, the real world detectors have limited sensitivity and, as a result, produce distorted peaks for highly absorptive analytes.

To solve the problem, we are proposing a nonlinear modification of the MCR-ALS method and call this technique *nonlinear MCR-ALS* (NL-MCR-ALS). The performance of NL-MCR-ALS is compared with PLS, classical MCR-ALS, and MCR-ALS with nonlinear correlation constraint. For this purpose, we use two data sets. The first one is simulated by means of one-peak spectra. Varying the dataset properties, we investigate various features of the method.

The second example describes the determination of a nitric acid concentration with the help of UV–Vis spectroscopy. Despite the apparent simplicity of the latter example, quantitative determination of nitric acid concentration using a spectrophotometer is a rather complex problem, as an aqueous solution of HNO<sub>3</sub> has no absorbance peaks in visual region. At the same time, nitric acid is widely used in various production processes, where the in-line control of HNO<sub>3</sub> concentration is vital. To compare the robustness of the models, the test set concentration ranges are selected to be wider than those for calibration subsets.

## 2. THEORY

### 2.1. Conventional methods

Partial least squares [9] is a well-known method of calibration; therefore, it will not be explained here in detail. In this paper, it is used for the comparison of calibration and prediction results with a newly developed method. For each dataset, two PLS models are established. The first (full) model uses the entire spectral range. In the second (short) model, the spectral range is reduced by the exclusion of peak saturation areas. The number of the PLS latent variables is determined in a common way, using the root mean squared errors (RMSE) of calibration, RMSEC, and prediction, RMSEP, which are calculated using the following formula:

$$\text{RMSE} = \sqrt{\frac{1}{I} \sum_{i=1}^I (c_i - \hat{c}_i)^2} / I \quad (1)$$

where  $c_i$  are the reference concentration values,  $\hat{c}_i$  are the estimated values, and  $I$  is the number of samples.

Another well-known method is MCR-ALS [3] that assumes a bilinear model:

$$\mathbf{X} = \mathbf{C}\mathbf{S}^t + \mathbf{E} \quad (2)$$

Here,  $\mathbf{X}$  is the  $(I \times J)$  matrix that contains spectra of  $I$  samples recorded for  $J$  wavelengths.  $\mathbf{C}$  is the  $(I \times N)$  matrix of the concentrations of pure components, and  $\mathbf{S}$  is the  $(J \times N)$  matrix of pure spectra.  $N$  is the number of components in the system.  $\mathbf{E}$  is the  $(I \times J)$  matrix, which contains variations not explained by the model.

There are two preliminary steps that are usually necessary for MCR-ALS. The first one involves the determination of the number of pure components  $N$ . This can be carried out by means of the principal component analysis, or applying any other similar procedure [10]. The second preliminary step includes evaluation of the initial estimate of  $\mathbf{S}$ , or  $\mathbf{C}$  to start the ALS procedure [4]. Afterwards, the matrices  $\mathbf{C}$  and  $\mathbf{S}$  are found in order by minimizing the sum of the squared residuals:

$$\text{minimize } \|\mathbf{X} - \mathbf{C}\mathbf{S}^t\|^2 \quad (3)$$

The ALS algorithm consists of the C-type step and the S-type step, which are repeated until convergence. At the C-type step, the value of  $\mathbf{S} \equiv \mathbf{S}_{\text{hat}}$  is fixed, and the  $\mathbf{C}$  matrix is calculated using the unconstrained least squares (LS) estimator:

$$\mathbf{C}_{\text{in}} = \mathbf{X}\mathbf{S}_{\text{hat}}^t (\mathbf{S}_{\text{hat}}^t \mathbf{S}_{\text{hat}})^{-1} \quad (4)$$

For the S-type step, the value of  $\mathbf{C} \equiv \mathbf{C}_{\text{hat}}$  is fixed, and matrix  $\mathbf{S}$  is found applying a similar formula:

$$\mathbf{S}_{\text{in}} = \mathbf{X}^t \mathbf{C}_{\text{hat}} (\mathbf{C}_{\text{hat}}^t \mathbf{C}_{\text{hat}})^{-1} \quad (5)$$

To give a physicochemical meaning to the LS estimates, certain necessary constraints are imposed at each step. For instance, there are natural nonnegativity constraints that force the concentration and spectra to be equal to or greater than zero. In calibration problems, additional correlation constraints [5] are applied. They are based on regressions that relate the known reference concentration matrix,  $\mathbf{C}_{\text{ref}}$ , with matrix  $\mathbf{C}_{\text{in}}$  obtained in the ALS procedure using Eq. (4):

$$\mathbf{C}_{\text{ref}} = \mathbf{A}\mathbf{C}_{\text{in}} + \mathbf{B} \quad (6)$$

Here,  $\mathbf{A}$  is the  $(N \times N)$  matrix of slopes, and  $\mathbf{B}$  is the  $(N \times N)$  matrix of intercepts [5]. In a simple case, a univariate regression  $\mathbf{C}_{n,\text{ref}} = a_n \mathbf{c}_{n,\text{in}} + b_n$  is developed for each component concentration vector  $\mathbf{c}_n$  [7]. Then,  $\mathbf{A} = \text{diag}(a_1, \dots, a_n)$ , and  $\mathbf{B} = (b_1 \mathbf{1}, \dots, b_n \mathbf{1})$ , where  $\mathbf{1}$  is the  $(N \times 1)$  vector of units.

The estimated regression matrices  $\mathbf{A}$  and  $\mathbf{B}$  are used to adjust matrix  $\mathbf{C}_{\text{hat}}$  by the following formula:

$$\mathbf{C}_{\text{hat}} = \mathbf{A}\mathbf{C}_{\text{in}} + \mathbf{B} \quad (7)$$

### 2.2. Peak saturation modeling

As discussed earlier, bands with high absorbance produce saturated spectra. This causes a loss of linearity between the peak height and concentration. While analyzing the UV–Vis spectra with saturated peaks, we have noticed that it is often rather difficult to distinguish between a well-measured peak and a saturated one. Only an additional experiment that involves sample dilution may reveal this, as saturated peaks acquired by instruments do not often have a pronounced flat top (Figure 1, left panel, curve 2). The shape of flattening depends on many factors. In diffraction spectrophotometers, it is primarily determined by the width of the optical slit [8]. In Fourier spectrometers, it depends on the algorithm used for spectrum

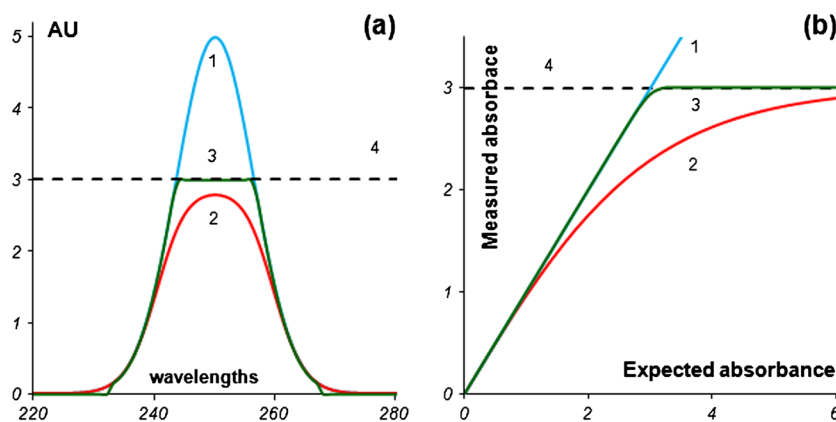


**Figure 1.** Peak saturation modeling for saturation level  $s = 3$  (4). The left panel (a) shows saturated peaks. Ideal case (1),  $p = 1$  (2), and  $p = 12$  (3). The right panel (b) shows corresponding transition functions.

digitalization. That is why, in general, spectrometers produce saturated peaks with flatter tops than spectrophotometers.

To account for such variations in the shape of saturated peaks, we introduce an empirical transition function given by the following formula:

$$\{x\}_{s,p} = s \left[ \tanh\left(\frac{x^p}{s^p}\right) \right]^{1/p} \quad (8)$$

Here,  $x$  is an ideal peak and  $\{x\}_{s,p}$  is its saturated modification. Function  $\tanh()$  stands for the hyperbolic tangent,  $p$  is the parameter that changes the peak shape, and  $s$  is the saturation level, that is, the upper value above which an instrument cannot measure absorbance accurately. Most of the commercially available instruments have  $s \leq 3$  AU. However, some spectrometers have been reported [11] to be stable up to 8 AU.

The right panel of Figure 1 presents transition functions given by Eq. (8) for different values of parameter  $p$ . The left panel shows corresponding saturated peaks, obtained by these functions. The saturation level is 3 AU. The transition function  $\{x\}_{s,p}$  possesses the following evident properties. At small absorbance values ( $x < s$ ), it is close to the diagonal  $\{x\}_{s,p} = x$ , and at large absorbance values ( $x > s$ ), it assumes a constant value  $\{x\}_{s,p} = s$ . In the proximity of the transition area ( $x \approx s$ ), the function form is defined by parameter  $p$ : The larger the parameter, the sharper the transition.

In our opinion, a specific form of the transition function (Eq.(8) is an example) is not so important. Any other function that meets the aforementioned conditions (diagonal at small  $x$ , constant at large  $x$ , etc.) will provide a similar result. This is because the function is used for the interpolation (not extrapolation!) purposes. Parameters  $s$  and  $p$  reflect the properties of a specific instrument. They depend on the measurement layout, instrument setup, tunings, and so on. Thus, ideally, parameters  $s$  and  $p$  should be evaluated a priori, using standard samples with well-established ideal spectra. However, in practice, the parameters can be found by optimization.

### 2.3. Novel methods

In the MCR-ALS method, the peak saturation primarily manifests itself through a nonlinear dependence between the  $C_{in}$  and  $C_{ref}$  values. An example is shown in Figure 2, which presents nitric acid calibration (the second case study, Section 4). The

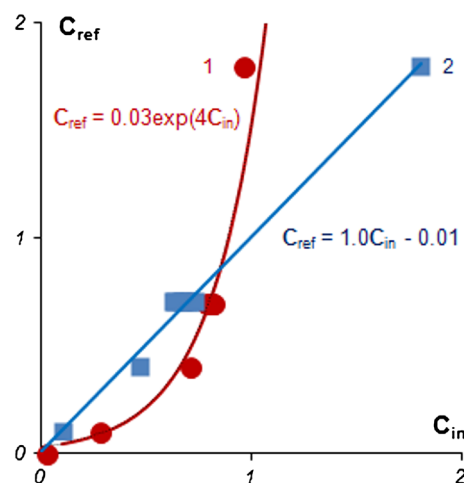


**Figure 2.** Nitric acid data. Relation between  $C_{in}$  and  $C_{ref}$ . Points set 1 is calculated by multivariate curve resolution alternating least squares (MCR-ALS); points set 2 is calculated by nonlinear MCR-ALS.

conventional MCR-ALS calibration produces points set 1, which should but cannot be fitted by a linear regression. Here, it seems natural to replace a linear regression given by Eq. (6), with a nonlinear one, for example, with a polynomial or exponential regression as shown by curve 1 in Figure 2. This method (labeled from now as MCR-ALS-NC) is studied in the subsequent sections. However, the approach is misleading, as the  $C_{ref}/C_{in}$  dependence has an evident singular point located near the concentration value that provides peak saturation. Unfortunately, the location of this point is difficult to predict.

The most prospective approach for analysis of peak saturated data is based on the following equation:

$$\mathbf{X} = \{\mathbf{CS}^t\}_{s,p} + \mathbf{E} \quad (9)$$

which contains nonlinear element-wise spectra mapping  $\{s,p\}$  defined by Eq. (8). Clearly, the linear LS method cannot be used to solve Eq. (9), and we arrive at a nonlinear optimization problem:

$$\underset{C,S}{\text{minimize}} \quad \|\mathbf{X} - \{\mathbf{CS}^t\}_{s,p}\|^2 \quad (10)$$

which solution can be obtained using the following modified ALS algorithm.

The C step (compare with Eq. (4)) is now presented by a problem:

$$\underset{\mathbf{C}}{\text{minimize}} \quad \|\mathbf{X} - \{\mathbf{CS}^t\}_{s,p}\|^2 \quad \text{subject to } \mathbf{S} = \mathbf{S}_{\text{hat}} \quad (11)$$

The S step (Eq.(5)) is performed via optimization:

$$\underset{\mathbf{S}}{\text{minimize}} \quad \|\mathbf{X} - \{\mathbf{CS}^t\}_{s,p}\|^2 \quad \text{subject to } \mathbf{C} = \mathbf{C}_{\text{hat}} \quad (12)$$

The correlation constraint presented by Eq. (6), where  $\mathbf{C}_{\text{in}}$  is now a solution of the problem given by Eq.(11), can be used more effectively. Figure 2 (points set 2) shows that the nonlinear mapping linearizes correlation between  $\mathbf{C}_{\text{ref}}$  and  $\mathbf{C}_{\text{in}}$ . Other constraints (nonnegativity, unimodality, etc.) for concentrations and spectra are also very important in the nonlinear case. These constraints may be applied in the same manner as in the classical procedure or can be included into the nonlinear optimization procedure.

In some aspects, the proposed method is very similar to the conventional MCR-ALS. The latter approach estimates matrices  $\mathbf{C}$  and  $\mathbf{S}$  whose product  $\mathbf{CS}^t$  fits matrix  $\mathbf{X}$  better. The nonlinear MCR-ALS also seeks for the same matrices  $\mathbf{C}$  and  $\mathbf{S}$ , but the aim is to fit in the *saturated product*  $\{\mathbf{CS}^t\}$  with matrix  $\mathbf{X}$ . Its algorithm is presented in the APPENDIX.

## 2.4. Computing

Nonlinear optimization can be a complex task, especially at the S step, where the size of sought spectra ( $J$ ) can be very large, for example,  $J=10\,000$  wavelengths. It may be advantageous to parameterize vector  $\mathbf{S}$  using a linear combination of Gaussian (or other) peaks. Therefore, we consider two versions of optimization in Eq. (12): global and parameterized. In global optimization, the dimension of the search space is equal to  $J$ . In the parameterized version, the dimension is  $M \cdot G$ , where  $M$  is the number of peaks, and  $G$  is the number of peak parameters. For the Gaussian shape,  $G$  is equal to 3.

As mentioned earlier, the nonlinear optimization in NL-MCR-ALS can be executed in two different ways. The first option employs an unconstrained optimization procedure with subsequent application of nonnegativity constraints in the same way as it is carried out in classical MCR-ALS. This approach is utilized for the second case study using the standard Excel Solver tool and Chemometrics Add-In [12].

The second option involves constrained nonlinear optimization. The nonnegativity constraints are used for  $\mathbf{C}$  and  $\mathbf{S}$  matrices. We test three optimization procedures from the MATLAB Optimization Toolbox. They are sequential quadratic programming, active set algorithm, and the interior point method [13,14]. The first two algorithms are designed to solve medium-scale problems, whereas the latter one is preferable for large-scale problems. Data processing for the first case was carried by means of in-house written routines.

## 3. SIMULATED EXAMPLE

### 3.1. Data set

The UV absorbance spectra in 240–300 nm range are simulated with the help of the Gaussian function:

$$S = C \exp(-z^2), \quad \text{where } z = (\lambda - 270)/8 \quad (13)$$

Here,  $C$  stands for concentration and varies from 0.1 to 8;  $\lambda$  denotes the wavelength value. In total, 17 samples are simulated. The number of wavelengths,  $J$ , in each spectrum is equal to 31. The simulated spectra are transformed using the transition function given in Eq. (8) with  $p=12$  (flat top) and with various saturation limits  $s$ . To simulate instrumental errors, pseudorandom normal noise with standard deviation of 0.2 is added. Finally, all negative values in the spectra profiles are substituted by zero values.

This example is used to explore the feasibility of the proposed method. The whole dataset is divided into the training subset ( $C=0.1, 1.0, 2.0, 2.5, 3.0, 3.5, 5.0, 5.5, 6.0$ ) and the test subset ( $C=0.5, 1.5, 4.0, 4.5, 6.5, 7.0, 7.5, 8.0$ ), which are shown in Figure 3.

### 3.2. Calibration and prediction

In this example, NL-MCR-ALS is used without parameterization, as spectrum  $\mathbf{S}$  is of a small size. The method provides good recovery of the pure spectrum. This is illustrated in Figure 4(a) by comparing the 'true' (simulated) spectrum, curve 1, and spectrum, resolved by the new method, curve 2.

Errors in calibration and prediction are also very small (Table I, last column). It is important to mention that the prediction versus reference plot (Figure 4(b)) demonstrates linear behavior for the concentrations predicted by NL-MCR-ALS in the whole

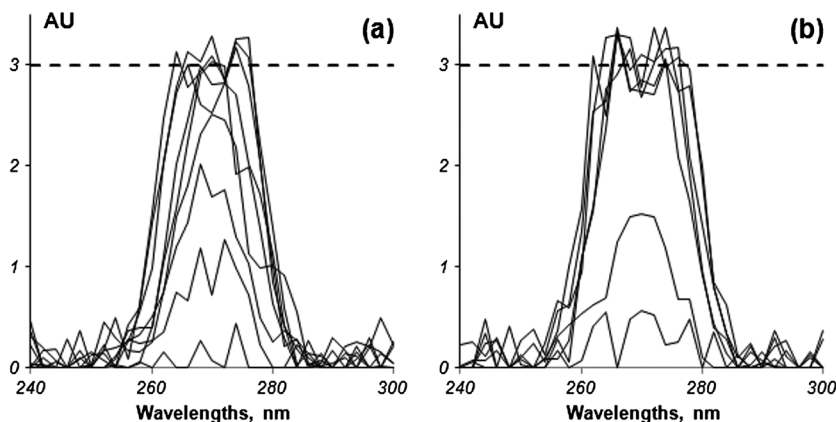
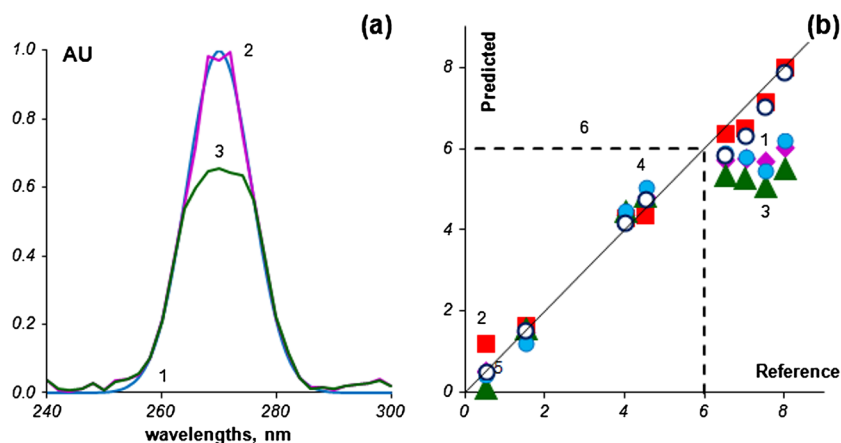


Figure 3. Simulated example, saturation level,  $s=3$ . Training set (a) and test set (b).



**Figure 4.** Simulated example. Left panel (a) shows initial (1) and reconstructed spectra: (2) by nonlinear multivariate curve resolution alternating least squares (NL-MCR-ALS) and (3) by MCR-ALS. Right panel (b) shows predictions by different methods: (1, ♦) full partial least squares (PLS), (2, ■) short PLS, (3, ▲) MCR-ALS, (4, ●) MCR-ALS-NC, (5, ○) nonlinear MCR-ALS, and (6) calibration area.

**Table I.** Simulated example (comparison of methods' performance)

	Full PLS (four PC)	Short PLS (two PC)	MCR-ALS	MCR-ALS-NC	NL-MCR-ALS
RMSEC	0.008	0.144	0.467	0.281	0.093
RMSEP	1.067	0.360	1.438	1.110	0.388

PLS, partial least squares; MCR-ALS, multivariate curve resolution alternating least squares; MCR-ALS-NC, multivariate curve resolution alternating least squares with non-linear constraints; NL-MCR-ALS, nonlinear multivariate curve resolution alternating least squares; RMSEC, root mean squared errors of calibration; RMSEP, root mean squared errors of prediction.

concentration range, even for the samples that have concentrations that are higher than those in the calibration set. This fact indicates the method stability and confirms its applicability for varying conditions in the PAT implementations.

The application of classical MCR-ALS with linear constraint delivers worse results. The recovered pure spectrum (Figure 4(a), curve 3) has a proper peak position, but the peak's height is low. An essential nonlinearity can be seen in the prediction versus reference plot, and the errors in calibration and prediction are notably higher than those for NL-MCR-ALS (Table I).

An attempt to take nonlinearity into account by introducing a nonlinear constraint in MCR-ALS does not help much. We tried using polynomial correlation constraints of a different order. The minimum of RMSEP is obtained for the fourth order, which is selected as optimal, but even in this case, the results are about three times worse (see column MCR-ALS-NC in Table I) than those obtained by NL-MCR-ALS.

For comparison, the data is also subjected to the PLS method. Two PLS models are constructed. The full PLS model uses the entire spectral region. Four PLS components provide the lowest RMSEP value in an attempt to compensate for data nonlinearity. Here, the RMSEC is the lowest among all methods (Table I); however, the prediction error is comparable with classical MCR-ALS, and an essential nonlinearity is seen in the prediction versus reference plot in Figure 4(a). At the same time, in this simulated example, it is easy to select the variable ranges where bilinearity is not violated. The two-factor short PLS model based on the composite variable range of 240–263 nm and 279–300 nm provides prediction results comparable with those of NL-MCR-ALS.

Thus, we can conclude that the prediction ability of the newly proposed NL-MCR-ALS method is comparable with that

of PLS in case special regions without violation of bilinearity exist in data. Otherwise, NL-MCR-ALS overperforms the aforementioned methods.

### 3.3. Experiments with simulated data

In order to better understand the behavior of the NL-MCR-ALS method, we performed several experiments that involve varying the dataset features of the simulated data.

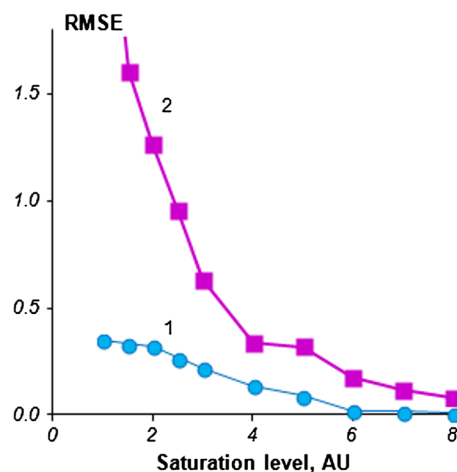


**Figure 5.** Simulated example. The root mean squared errors (RMSE) of calibration (1) and RMSE of prediction (2) values obtained by nonlinear multivariate curve resolution alternating least squares in relation to saturation level.

This article is protected by the copyright law. You may copy and distribute this article for your personal use only. Other uses are only allowed with written permission by the copyright holder.

First, we changed the saturation level from 0.5 to 8 AU aiming to assess the method's calibration/prediction abilities. It is clear that the wider the concentration range without peak flattening is, the more reliable a calibration/prediction will be obtained. The maximal saturation level of 8 AU corresponds to the case when all spectra are not saturated. The quality of modeling by NL-MCR-ALS is shown in Figure 5. From the presented results, we can conclude that reasonable outcomes (RMSEC=0.32 and RMSEP=1.27) are obtained at the saturation level of 2 AU. This means that at least one unsaturated spectrum should be included in the calibration set for successful reconstruction of the pure spectra. The predictive ability of the model improves

**Table II.** Simulated example (nonlinear optimization algorithms' performance)

Number of wavelengths	Time (s)		
	Interior point	SQP	Active set
31	<3	<5	<2
61	<3	<5	<2
121	<3	<5	2
301	<3	5	16
601	3	22	92
1201	5	193	432
2401	12	2164	>3000

SQP, sequential quadratic programming.

**Table III.** Nitric acid data (samples used for analysis)

Samples		HNO <sub>3</sub> concentration mol/l (=M)
Training	Test	
1	0	0
1	1	0.1
1	1	0.4
7	1	0.7
1	1	1.8
0	1	3.0
0	1	4.0

exponentially when the saturation level is increased. This means that NL-MCR-ALS works well when bilinearity is not violated. Naturally, if this is the case, less computationally cumbersome methods are preferable.

The second answer we seek is the speed of different optimization procedures. The goal of the experiment is to understand whether the dimensionality of initial data matrix can be a barrier for the NL-MCR-ALS application. For this purpose, we simulated data with increasing spectra resolution in the range 240–300 nm. The number of wavelengths/variables and corresponding computing time of all the aforementioned algorithms (Section 2.4) are presented in Table II.

The first and expected conclusion is that an algorithm designed for solving large-scale problems such as the interior point procedure works noticeably quicker than the other two algorithms. At the same time, we recognize that the search for the most effective, in terms of speed performance and accuracy, algorithm should be continued. The main conclusion derived from this study is that application of the nonlinear optimization procedure is not a computational obstacle for the implementation of the NL-MCR-ALS method.

## 4. NITRIC ACID DETERMINATION

### 4.1. Data set

Concentrated nitric acid with a density of 1.35 g/ml and distilled water are used for preparation of 18 samples of aqueous solution of HNO<sub>3</sub> with various concentrations (Table III). The samples are subjected to the UV-Vis spectroscopy in the transmittance mode and then converted to the absorbance units. Data are collected with a wavelength increment of 1 nm among consecutive measurements over the range of 200–1000 nm using the spectrophotometer UNICO SQ-2800 with the photometric range of 0.01–3 AU. A 10 mm path length quartz cuvette is used. As HNO<sub>3</sub> has no absorbance peaks in visual region, only the range of 200–350 nm is considered.

The spectra are shown in Figure 6.

### 4.2. Calibration and prediction

Nitric acid has two strong absorbance peaks around 247 and 295 nm. The saturation level defined by the instrument is  $s=3$  AU. Among the acquired spectra, only samples with

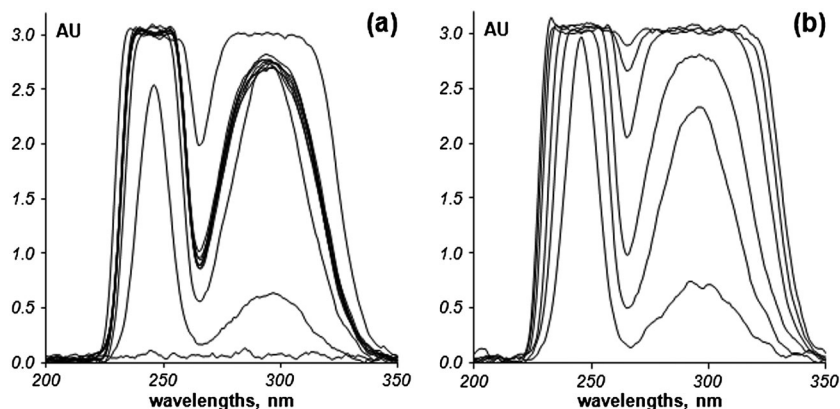


**Figure 6.** Nitric acid data. Absorbance spectra of nitric acid; training set (a) and test set (b).

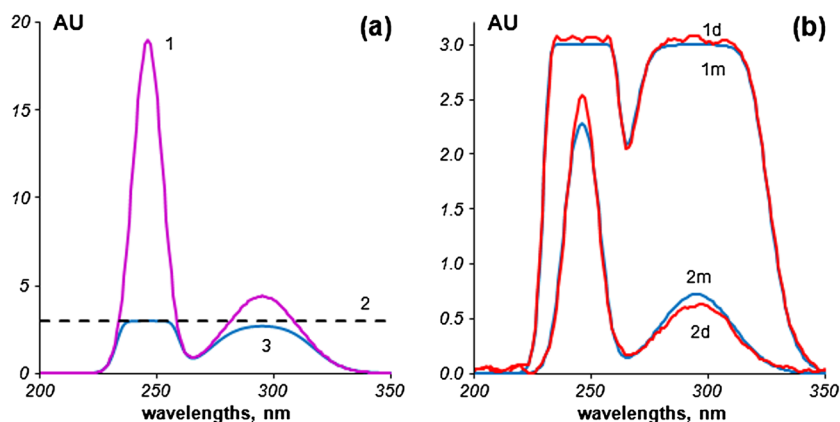


**Figure 7.** Nonlinear multivariate curve resolution alternating least squares for nitric acid data. Left panel (a): ideal (1) and saturated spectra (3) of HNO<sub>3</sub> at concentration 0.7 M. Saturation level (2). Right panel (b): measured (1d, 2d) and modeled (1m, 2m) spectra for HNO<sub>3</sub> concentrations: 1.8 M (1d, 1m) and 0.1 M (2d, 2m).

**Table IV.** Comparison of methods' performance in determination of HNO<sub>3</sub> concentrations

	Full PLS (five PC)	Short PLS (three PC)	MCR-ALS	MCR-ALS-NC	NL-MCR-ALS
RMSEC	0.01	0.03	0.27	0.14	0.04
RMSEP	0.52	0.13	1.47	1.10	0.09

PLS, partial least squares; MCR-ALS, multivariate curve resolution alternating least squares; MCR-ALS-NC, multivariate curve resolution alternating least squares with non-linear constraints; NL-MCR-ALS, nonlinear multivariate curve resolution alternating least squares; RMSEC, root mean squared errors of calibration; RMSEP, root mean squared errors of prediction.

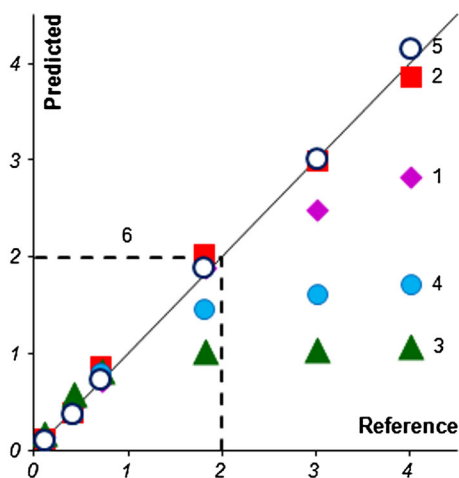


**Figure 8.** Prediction of HNO<sub>3</sub> concentration by different methods: (1, ◆) full partial least squares (PLS), (2, ■) short PLS, (3, ▲) multivariate curve resolution alternating least squares (MCR-ALS), (4, ●) MCR-ALS with non-linear constraints MCR-ALS-NC, (5, ○) nonlinear MCR-ALS, and (6) calibration area.

concentration of 0.1 M have spectra without flattening effect for both peaks.

The spectra are parameterized using two Gaussian peaks. The transition function given by Eq.(8) with  $p=1$  is applied. The 'mechanism' of application of the transition function is shown in Figure 7(a). Figure 7(b) shows that the resolved spectra perfectly describe both saturated and unsaturated spectral peaks. An accurate prediction is obtained not only for test

samples with concentrations inside the calibration range but also for samples with higher concentrations. Thus, NL-MCR-ALS provides an accurate and stable model.

To assess the quantification performance of the new procedure, we compare it with the full range PLS, the short range (200–226, 321–350 nm) PLS, a conventional MCR-ALS, and MCR-ALS-NC. The results are presented in Table IV and Figure 8.

The prediction results for PLS established for the full spectral range and by conventional MCR-ALS are unsatisfactory. The loss of linearity can be clearly seen in Figures 2 and 8. Variable selection helps to establish a satisfactory short PLS model, as the composite range 200–226 nm together with 321–350 nm does not include flattened peaks, and at the same time carries useful information about analyte concentrations. MCR-ALS-NC is used with exponential (Figure 2) correlation constraint  $C_{ref} = \exp(aC_{in} + b)$ . It is obvious that such a constraint does not help much to manage the nonlinearity in prediction.

The RMSEP value provided by the NL-MCR-ALS is 50% lower than RMSEP obtained by the short PLS method. Figure 8 shows that these methods can manage the nonlinearity. The latter model is able to avoid nonlinearity by means of variables' selection, whereas NL-MCR-ALS does this with the help of saturated spectra modeling. It is important to emphasize that not only NL-MCR-ALS predicts the response but also reconstructs the pure component spectrum.

## 5. CONCLUSIONS

In this paper, we propose a novel method for nonlinear MCR based on a modified ALS algorithm (NL-MCR-ALS) and intended

for data analysis when the bilinearity principle does not hold. The presented examples allow us to claim that the NL-MCR-ALS approach has evident advantages over the conventional methods, providing a better prediction accuracy for distorted data, which do not obey the Lambert–Beer law because of ‘peak flattening’. With respect to other nonlinear effects (scattering, Lorenz factor, etc.), it seems possible to use a similar approach:

$$\text{Real spectrum} = \text{Transition function (Ideal spectrum)},$$

for data modeling. Certainly, transition functions should be developed to account for a specific nonlinearity. This is just a suggestion that needs a more detailed elaboration.

A surprising result is that PLS method with a proper variable selection procedure is the only worthy adversary. This can be explained by the fact that in such simple cases, some traces of linearity are still preserved at the edges of the spectral range. In more complex cases, which are now ready for publication, PLS fails to manage the nonlinearity regardless of the range selected.

The main disadvantage of the advocated approach is that it requires a more complicated computing procedure that includes nonlinear optimization steps. We investigated several algorithms and discovered that the computation time is still reasonable, even for a large data set that includes thousands of variables. However, the question is still open, and the search for the most suitable optimization method goes on. By and large, the NL-MCR-ALS method is not yet fully investigated, and many more efforts should be undertaken to better understand its pros and cons. In the succeeding texts are a few examples of the forthcoming tasks. As we deal with nonlinear problems, it should be interesting to compare the results yielded by NL-MCR-ALS with those provided by other nonlinear approaches, for example, kernel methods [15]. It is important to evaluate the NL-MCR-ALS capabilities in quantification of complex mixtures, as well as analyze the method’s performance when other sources of nonlinearity are present in the system. From a calculation point of view, it is interesting to investigate the influence of various types of spectra parameterization on the speed of convergence and on the accuracy of final results. We should keep in mind that parameterization of the concentration profiles is also possible in the frame of NL-MCR-ALS. Such an approach can link the proposed procedure to kinetic modeling [16].

It should be emphasized that the anticipated approach helps to extend the capabilities of spectroscopic instruments by tuning a spectrometer for analysis of specific manufacturing processes and to broaden the PAT solutions.

## REFERENCES

- Pomerantsev AL, Ye O, Rodionova. Process analytical technology: a critical view of the chemometricians. *J. Chemom.* 2012; **26**: 299–310.
- Naes T, Isaksson T, Fearn T, Davies T. *Multivariate Calibration and Classification*, Wiley: Chichester, 2002.
- de Juan A, Tauler R. Multivariate curve resolution (MCR) from 2000: progress in concepts and applications. *Crit. Rev. Anal. Chem.* 2006; **36**: 163.
- de Juan A, Rutan SC, Maeder M, Tauler R. Multivariate curve resolution chapters. In *Comprehensive Chemometrics*, vol. **2**. Brown D, Tauler R, Walczak B (eds.). Elsevier: Amsterdam, 2009; 325–344, 473–506.
- de Oliveira RR, de Lima KMG, Tauler R, de Juan A. Application of correlation constrained multivariate curve resolution alternating least-squares methods for determination of compounds of interest in biodiesel blends using NIR and UV–visible spectroscopic data. *Talanta* 2014; **125**: 233–241.

- Antunes MC, Simao JEJ, Duarte AC, Tauler R. Multivariate curve resolution of overlapping voltammetric peaks: quantitative analysis of binary and quaternary metal mixtures. *Analyst* 2002; **127**(6): 809.
- Azzouz T, Tauler R. Application of multivariate curve resolution alternating least squares (MCR-ALS) to the quantitative analysis of pharmaceutical and agricultural samples. *Talanta* 2008; **74**: 1201–1210.
- Skoog D, Holler FJ, Crouch SR. *Principles of Instrumental Analysis*, Brooks Cole: Belmont, CA, 2007.
- Wold S, Sjostroma M, Eriksson L. PLS-regression: a basic tool of chemometrics. *Chemom. Intell. Lab. Syst.* 2001; **58**: 109–130.
- Maeder M. Evolving factor analysis for the resolution of overlapping chromatographic peaks. *Anal. Chem.* 1987; **59**(3): 527–530.
- <http://www.perkinelmer.com/catalog/product/id/L950>
- Pomerantsev AL. *Chemometrics in Excel*, John Wiley & Sons: Hoboken NJ, 2014.
- Fletcher R. *Practical Methods of Optimization*, John Wiley & Sons: Chichester, 1987.
- Dantzig GB, Thapa MN. *Linear Programming 2: Theory and Extensions*, Springer-Verlag: NY, 2003.
- Suykens J. Kernel methods. In *Comprehensive Chemometrics* vol. **3**, Brown D, Tauler R, Walczak B (eds.). Elsevier: Amsterdam, 2009; 437–450.
- Diewok J, de Juan A, Maeder M, Tauler R, Lendl B. Application of a combination of hard and soft modeling for equilibrium systems to the quantitative analysis of pH-modulated mixture samples. *Anal. Chem.* 2003; **75**: 641–647.

## APPENDIX. NL-MCR-ALS ALGORITHM

The algorithm consists of two parts: calibration stage and prediction stage. The first part is executed iteratively, the second part takes one step. For better understanding of the algorithm, one should refer the definition of  $\{s,p\}$  given by Eq. (8). Matrix operation  $\mathbf{X} = \max(\mathbf{Y}, \mathbf{Z})$  means the element-wise selection, that is,  $x_{ij} = \max(y_{ij}, z_{ij})$ .

### Calibration stage

Given:

$\mathbf{X}_c$  is the calibration ( $I \times J$ ) data matrix.

$N$  is the number of components of the analyzed mixture.

$s$  is the saturation level defined by a specific instrument.

$p$  is the parameter that defines the form of the transition function constraints defined by the specific problem.

### Initialization step

$\mathbf{S}_{\text{hat}}$  is the initial pure spectra matrix ( $J \times N$ ).

$\mathbf{C}_{\text{hat}}$  is the initial concentration matrix ( $I \times N$ ).

(1) S step calculation

Find  $\mathbf{S}_{\text{in}}$  such that minimizes  $\|\mathbf{X}_c - \{\mathbf{CS}_{\text{in}}\}_{s,p}\|^2$ , subject to  $\mathbf{C} \equiv \mathbf{C}_{\text{hat}}$ .

(2) Adjustment of  $\mathbf{S}$

Transform  $\mathbf{S}_{\text{in}}$  into  $\mathbf{S}_{\text{hat}}$  to incorporate the constraints, for example,  $\mathbf{S}_{\text{hat}} = \max(\mathbf{0}, \mathbf{S}_{\text{in}})$ .

(3) C step calculation

Find  $\mathbf{C}_{\text{in}}$  such that minimizes  $\|\mathbf{X}_c - \{\mathbf{CS}_{\text{in}}\}_{s,p}\|^2$ , subject to  $\mathbf{S} \equiv \mathbf{S}_{\text{hat}}$ .

(4) Correlation constraint

Estimate matrices  $\mathbf{A}$  and  $\mathbf{B}$  in the regression  $\mathbf{C}_{\text{ref}} = \mathbf{AC}_{\text{in}} + \mathbf{B}$ .

(5) Adjustment of  $\mathbf{C}$

Transform  $\mathbf{C}_{\text{in}}$  into  $\mathbf{C}_{\text{hat}}$  to incorporate the constraint, for example,  $\mathbf{C}_{\text{hat}} = \max(\mathbf{0}, \mathbf{AC}_{\text{in}} + \mathbf{B})$ .

(6) Return to step 1 until convergence.

**Prediction stage**

Given:

$\mathbf{X}_t$  is the  $(I_t \times J)$  data matrix of new or test samples.

**Obtained (from the calibration stage):**

$\mathbf{S}_{\text{hat}}$  is the pure spectra  $(J \times N)$  matrix.

$\mathbf{A}$  and  $\mathbf{B}$  are the correlation parameters.

$s$  is the saturation level.

$p$  is the form parameter.

(1) C step calculation

Find  $\mathbf{C}_{\text{in}}$  such that minimizes  $\|\mathbf{X}_t - \{\mathbf{CS}\}_{s,p}\|^2$ , subject to  $\mathbf{S} \equiv \mathbf{S}_{\text{hat}}$ .

(2) Adjustment of  $\mathbf{C}$

Transform  $\mathbf{C}_{\text{in}}$  into  $\mathbf{C}_{\text{hat}}$  to incorporate the constrains, for example,  $\mathbf{C}_{\text{hat}} = \max(\mathbf{0}, \mathbf{AC}_{\text{in}} + \mathbf{B})$ .

**Result:**

$\mathbf{C}_{\text{hat}}$  is the  $(I_t \times N)$  matrix of concentrations of new/test samples.